CHEMICAL ENGINEERING TRANSACTIONS
VOL. 41, 2014
A publication of AIDIC
The Italian Association of Chemical Engineering
www.aidic.it/cet
Guest Editors: Simonetta Palmas, Michele Mascia, Annalisa Vacca

ISBN 978-88-95608-32-7; **ISSN** 2283-9216
DOI: 10.3303/CET1441037

Synthesis and Characterization of Electrocatalyticgraphene/MoS2/Ni Nanocomposites

Maria Sarno*, Claudia Cirillo, Anna Garamella, Paolo Ciambelli

Department of Industrial Engineering and Centre NANO_MATES, University of Salerno
Via Giovanni Paolo II ,132 - 84084 Fisciano (SA), Italy
msarno@unisa.it

NiMoS nanohybrid, consisting in nanosheets of MoS_2 mainly covering nanoparticles of NiS, capped by an oleylamine/oleic acid organic coating, has been successfully synthesized, on few layer graphene (FLG) obtained by physical exfoliation of graphite, by thermolysis of suitable precursors in organic solvent in the presence of surfactants. The samples were characterized by Raman Spectroscopy, Electron Microscopy, and X-ray diffraction, and tested for HER activity using a typical three-electrode setup.
We obtained excellent HER activity, with a Tafel slope of 45 mV/dec compatible with electrochemical desorption as rate limiting step and high current density values.

1. Introduction

Carbon materials are widely used supports for dispersing catalytic metal nanoparticles, due to their high surface area, effective porous structure for transferring reactants and products, good electrical conductivity required for electrochemical reactions (Kou et al., 2011) and energy application (Li et al., 2011). Graphene sheets have been used as template to deposit metal catalysts for electrocatalysis and as building blocks to form metal/graphene supports for catalysts and battery applications (Zhao et al., 2013). On the other hand, MoS_2 is a promising catalyst for electrocatalytic or photocatalytic hydrogen evolution reaction (HER) in aqueous solution (Sarno et al., 2014b), nickel is often used as HER electrocatalyst (Popczun et al., 2013), also commercially.

Among the different methods to synthesize nanomaterials, one of the most promising is a “bottom-up” chemical strategy, offering many advantages, such as experimental easiness and potential low-cost fabrication (Altavilla et al., 2011; Altavilla et al., 2013). Here, we report a new one-step synthetic strategy for the preparation of few layer graphene (FLG)/NiMoS nanohybrid, consisting in nanosheets of MoS_2 laying on NiS nanoparticles, capped by an oleylamine/oleic acid organic coating, synthesized by thermal decomposition of precursors in organic solvent in the presence of surfactants, on graphene nanosheets obtained by physical exfoliation of graphite (Hernandez et al., 2008; Sarno et al., 2014a). All the samples obtained were characterized by Raman Spectroscopy, Scanning Electron Microscopy (SEM), Transmission Electron Microscopy – Energy dispersive X-ray spectroscopy (TEM-EDS), thermogravimetric analysis coupled with mass spectromery (TG-DTG-MS), X-ray diffraction (XRD), and tested for HER using a typical three-electrode setup. We found that our catalysts show excellent HER activity, Tafel slope of 45 mV/dec and high current density values.

2. Experimental

The synthesis was carried out using standard airless procedures and commercially available reagents. Ethanol (99.8%, Fluka) and hexane (>95%, Sigma-Aldrich) were used as received. Benzyl ether (99%), 1,2-hexadecanediol (97%), oleic acid (90%), oleylamine (70%), nickel (II) acetylacetonate (90%), 1-2-hexadecanediol (90%), ammonium tetrathiomolybdate (99.97% metal basis) were purchased from Aldrich. Graphite powder (microcrystalline, -300 mesh) was purchased from AlfaAesar.

Please cite this article as: Sarno M., Cirillo C., Garamella A., Ciambelli P., 2014, Synthesis and characterization of electrocatalyticgraphene/mos2/ni nanocomposites, Chemical Engineering Transactions, 41, 217-222 DOI: 10.3303/CET1441037

0.25 g of Nickel (II) acetylacetonate [$(C_5H_8O_2)_2Ni$], 0.25 g of ammonium tetrathiomolybdate [$(NH_4)_2MoS_4$)], 0.50 g of FLG, 10 mmol of 1,2-hexadecanediol, 6 mmol of oleic acid, 6 mmol of oleylamine, and 20 mL of benzyl ether were magnetically stirred under a flow of nitrogen. Few layer graphene (FLG) were obtained by a sonication of graphite in N-methylpyrrolidone (NMP, spectrophotometric grade> 99.0%) (cylindrical vial, 10-25 ml solvent) at a concentration of 10 mg/ml for 1 h at the maximum power of ultrasound (Sarno et al., 2014a, Sarno et al. 2013). FLG were recovered by vacuum filtration of the supernatant solution obtained after a suitable centrifugation (the supernatant contains about the 30 wt% of the original graphite -TG evaluation, not reported here), onto: porous alumina membranes (pore size: 20 nm).
The mixture was heated to 200°C for 2 h under nitrogen flow and then, under a blanket of nitrogen, heated to reflux (~ 300°C) for 1 h (see the scheme in Figure 1a). The black-colored mixture was cooled to room temperature by removing the heat source. Under ambient conditions, ethanol (40 mL) was added to the mixture, and a black material was precipitated and separated via centrifugation. The obtained product was dissolved in hexane. Centrifugation (10000 rpm, 10 min) was applied to remove any undispersed residue. The product, in the following NiMoS-FLG, was then precipitated with ethanol, centrifuged (10000 rpm, 10 min) to remove the solvent, and redispersed into hexane.
The characterization was obtained by the combined use of different techniques. Transmission electron microscopy (TEM) images were acquired using a FEI Tecnai electron microscope operated at 200 KV with a LaB6 filament as the source of electrons, equipped with an EDX probe. Scanning electron microscopy (SEM) images were obtained with a LEO 1525 microscope. Raman spectra were obtained at room temperature with a micro-Raman spectrometer Renishaw inVia with a 514 nm excitation wavelength (laser power 30 mW) in the range 100-3000 cm^{-1}. Optical images were collected with a Leica DMLM optical microscope connected on-line with the Raman instrument. For all the sample about 40 measurements have been carried out. The laser spot diameter was about 10 μm. XRD measurements were performed with a Bruker D8 X-ray diffractometer using Cu$K\alpha$ radiation. Thermogravimetric analysis (TG-DTG) at a 10 K/min heating rate in flowing air was performed with a SDTQ 600 Analyzer (TA Instruments) coupled with a mass spectrometer. For the electrochemical measurements 4 mg of catalyst were dispersed in 80 μl of 5 wt% Nafion solution to form a homogeneous ink. Then the catalyst ink was loaded onto a glassy carbon electrode of 3 mm in diameter. Linear sweep voltammetry (using the pontentiostat from Amel Instruments) with scan rate of 2 mVs^{-1} was conducted in 0.5 M H_2SO_4, using saturated calomel electrode as the reference electrode, a graphite electrode as the counter electrode and a loadable glassy carbon electrode as the working electrode.

3. Results and discussion

Nickel acetylacetonate reacts first with ammonium tetrathiomolybdate according to the following reaction (Alvarez et al., 2008; Pedraza et al., 2000):

$Ni(C_5H_8O_2)_2 + (NH_4)_2MoS_4 \rightarrow NiMoS_4[NH_4((C_5H_8O_2)]_2$

the reaction product first decomposes to give a NiMo sulphur reached phase, which later releases additional sulphur (Pedraza et al. 2000). In particular the two reaction steps has been followed during a thermogravimetric test by a mass spectrometer (Figure1b). The decomposition of the two precursors begins almost immediately, as clearly indicated by the corresponding total ion current (TIC) of the most intense mass fragments peaks: m/z = 27, 43, 58, 105 and 106 from acetylacetonate and m/z 17, 48 and 64 accounting for NH_3 and SO_2 release (which is formed in the presence of oxygen coming from the decomposition of the other components).
In particular, NH_3 and SO_2 release continue along the isotherm, with a further well identifiable contribution in correspondence of the second temperature increase. The solvents were chosen for the high boiling point, however, during the thermogravimetric analysis they in part leave the reaction zone, while under normal synthesis conditions this is controlled by reflux (see the scheme in Figure 1a). In particular, starting from the onset of the second temperature increase, 1,2-hexadecanediol release is observed, as clearly indicated by the corresponding total ion current (TIC) of the most intense mass fragments peaks: m/z 29, 43, 55, 67, 69, 81, 83, 97 and 98. Benzyl ether, which is the greater amount component, moves away along the whole isotherm phase and then during the further temperature increase and starting from 200°C (m/z 27, 39, 51, 63, 65, 79, 92).
On the other hand, the weight loss due to the release of the precursors volatile components is lower than the 1 wt.% total base. It can be not excluded that also a certain amount of oleic acid can move away from the thermobalance at high temperatures, where we can observe its main fragments (m/z 29, 41, 55, 69, 83, 97). While, already at lower temperatures, oleylamine release can be observed (m/z 30, 41, 55, 67, 81).

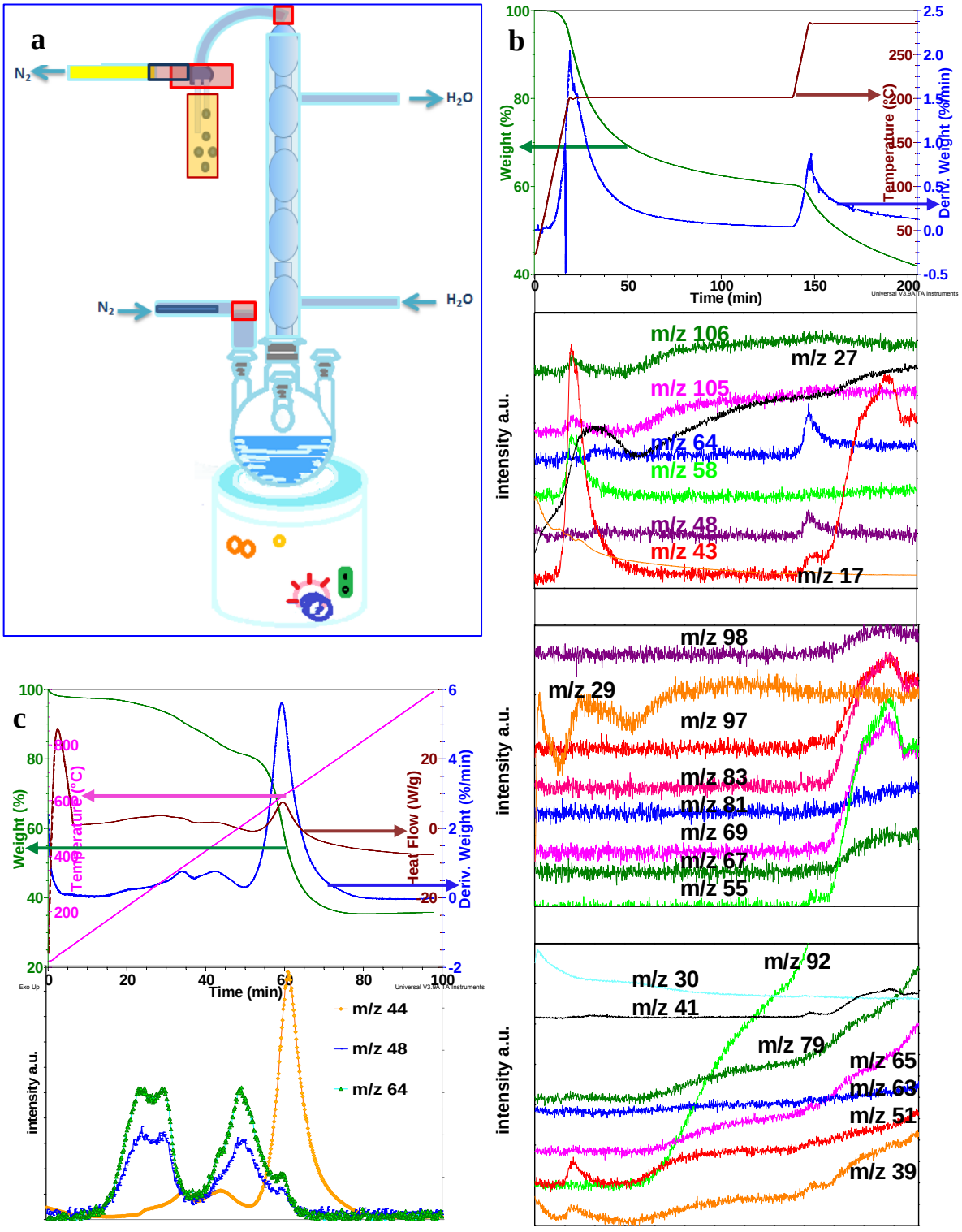

Figure 1. Experimental setup scheme (a). TG-DTG profiles, during the thermogravimetric test simulating the nanohybrid synthesis and the corresponding TIC (b). TG-DTG profiles, of the NiMoS-FLG nanohybrid and the corresponding TIC (c).

The thermal conversion of NiMoS-FLG in air flow occurred in three main weight loss steps (Figure 1c). The first one 8.5 wt.% is due to sulfur impurities (Altavilla 2011), oxidized during the TG measurements in air flow to SO_2, (see the SO_2 profile in the same temperature range of the weight loss) and to the starting oxidation of the NiMoS oleylamine/oleic acid organic capped hybrid system (onset temperature 220°C)

with exothermal (see the DSC profile in Figure 1c) release of SO_2 (m/s = 64) and CO_2 (m/s = 44) completing during the second loss step (onset 390°C). The last weight loss step (onset at 520°C) corresponds mainly to the oxidation of the FLG.

Figure 2 shows the diffraction pattern recorded on the reaction product, after a suitable washing, the patter has been obtained by subtracting the typical profile of FLG (Sarno et al., 2014b). All the sample is characterized by a low degree of crystallinity, $NiS_{1.03}$ and NiS (synthetic millerite) phases were observed (Pedraza et al., 2000), some of the typical MoS_2 peaks are barely visible.

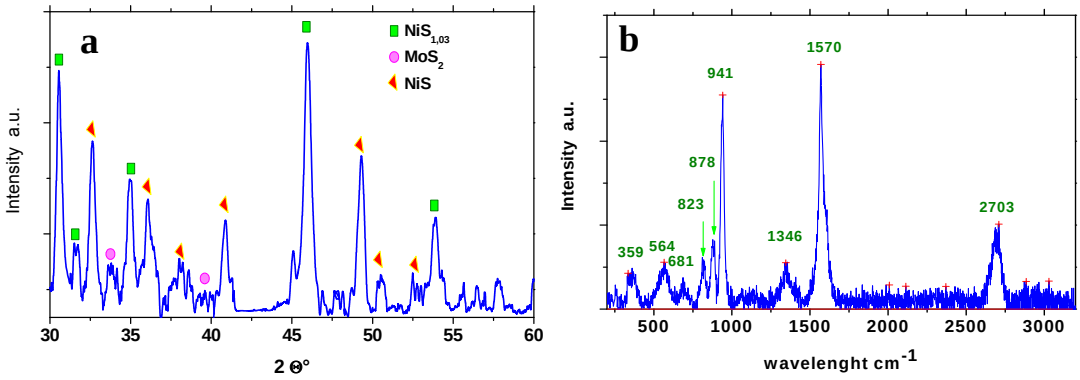

Figure 2. XRD patter of NiMoS (a). Raman Spectra of NiMoS-FLG in the range 200-3200 cm^{-1}(b).

Figure 2b shows a typical Raman spectrum of NiMoS-FLG excited by 514 nm line in air ambient environment. In the high wavelength range the typical spectrum of FLG is reported. The two most intense features are the G peak at ~1570 $cm^{-1}$and the 2D band at ~2700 cm^{-1} (Casiraghi et al., 2005), which differs from that typical for graphite, consisting of two components $2D_1$ and $2D_2$, the second with an highest intensity than the first, has a quite flat apex and can be easily deconvolved with almost two peaks. A broad D-band can be also seen, likely due to the FLG edges (taking into account the laser spot dimension and the flakes size (Sarno et al., 2014a). The bands at 681, 823, 878 and 941 cm^{-1} can be assigned to NiMo oxides generated by the laser, which photon energy closely resonant with the electronic absorption and the band gap energies, determines heating/photochemistry via direct absorption (Cervantes-Gaxiola et al., 2013). The typical Raman bands of NiS in the range 200-600 cm^{-1} (Guillaume et al., 2008) are also visible, probably covering or overlapping the A_{1g} and E'_{2g} modes for MoS_2 at about 382 and 407 cm^{-1} (Altavilla et al., 2013).

Figure 3a shows bright-field TEM images, at different magnifications of nanohybrid obtained. A lot of nanoparticles (Figure 3b and 3c) 10-15 nm in size, lying on FLG, are visible. FLG flakes have a lateral size of few micrometres. Most of the FLG sample consists of flakes with less than 6 sheets (85% ranging from 1 to 13), the number fraction of monolayer graphene (number of monolayers/total number of flakes observed) in NMP dispersions of 22%. In the sample a fraction of flakes (about 6% total based) with a number of sheets between 30 and 40, are also present (Sarno et al., 2014a). In particular, at increasing magnification, it is possible to observe nanoparticles partially covered by 1-2 MoS_2 layers (Figure 3d and 3e). In the sample free MoS_2 (indicated by the arrows in Figure 3f) can be also observed, in a very few cases with an higher number of layers, see Figure 3g, that constitute an enlargement of an area indicated by the arrows in Figure 3c. It is also possible to observe in Figure 3h the typical MoS_2 parallel lines laying on NiS nanoparticles with the typical interplanar spacing of 0.47 nm. The energy dispersive TEM based X-ray spectroscopy (EDS) not shown here confirms the Ni/Mo ratio ~ 1 .at, and the presence of an excess sulphur S/(Ni+Mo) ~ 1.8 .at.

We investigated the electrocatalytic HER activities of our hybrid material deposited on a glassy carbon electrode in 0.5 M H_2SO_4 solutions using a typical three-electrode setup (Figure 4a). As a reference point, we also measured a commercial Pt catalyst with high HER catalytic performances. Polarization curve (i-V plot) recorded with NiMoS-FLG showed an overpotential of ~0.12 V for HER, beyond which the cathodic current rose rapidly under more negative potentials. In sharp contrast FLG alone exhibited little HER activity. Linear portions of the Tafel plots (Figure 4b) were fit to the Tafel equation ($\eta = b \log j + a$, where η is the overpotential, j is the current density, b is the Tafel slope), yielding Tafel slopes of ~30 and ~45 mV/decade (iR-corrected) for Pt, and NiMoS–FLG hybrid, respectively.

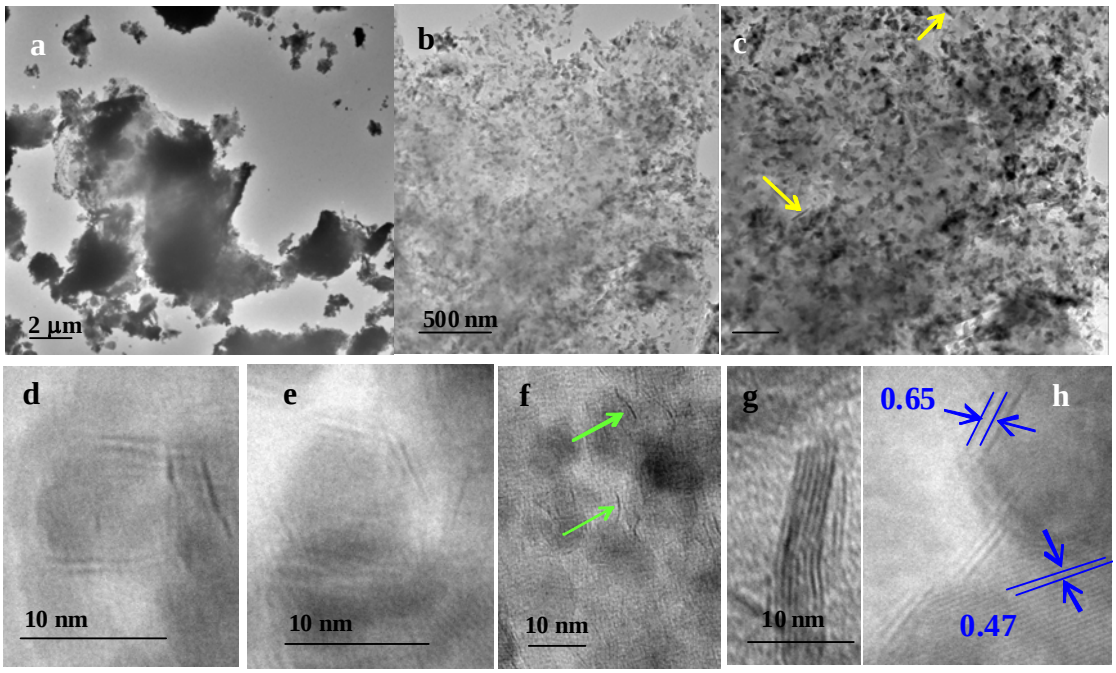

Figure 3. NiMoS-FLG TEM images at increasing magnification (a, b, c). The arrows in © indicate few thicker MoS2 sheets, one of which is magnified in the insert (g). High resolution TEM images (d, e, f, g, h).

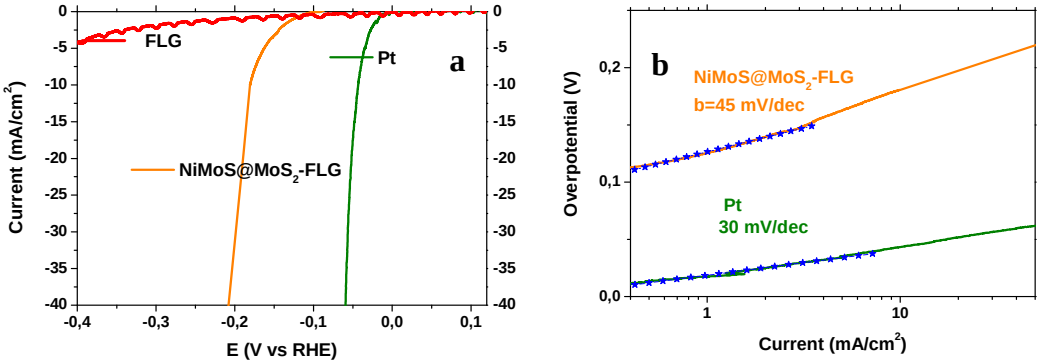

Figure 4. Polarization curves obtained with several catalyst as indicated (a), and corresponding Tafel plots recorded on glassy carbon electrodes (b).

The observed Tafel slope suggests that electrochemical desorption is the rate limiting step (Li et al., 2011), the high performance likely due to an electronic coupling between the FLG and the nanoparticles.

4. Conclusions

NiMoS nanohybrid, consisting in nanosheets of MoS_2 mainly covering nanoparticles of NiS and capped by an oleylamine/oleic acid organic coating, has been successfully synthesized, on few layer graphene (FLG) obtained by physical exfoliation of graphite, by thermolysis of suitable precursors in organic solvent in the presence of surfactants. The synthesis evolution has been monitored with a mass spectrometer under a thermogravimetric test, nickel acetylacetonate reacts first with ammonium tetrathiomolybdate, which decomposition begins almost immediately with the formation of NiS nanoparticles, ammonium tetrathiomolybdate decomposition products continue to release along the isotherm, with a further well identifiable contribution in correspondence of the second temperature increase and final formation of MoS_2. X-ray diffraction and Raman Spectroscopy confirms the nature of the product that show excellent HER activity, with a Tafel slope of 45 mV/dec compatible with electrochemical desorption as rate limiting step.

References

Altavilla C., Sarno M., Ciambelli P., 2011, A Novel Wet Chemistry Approach for the Synthesis of Hybrid 2D Free-Floating Single or Multilayer Nanosheets of MS2@oleylamine (M=Mo, W), Chem. Mater. 23, 3879-3885.

Altavilla C., Sarno M., Ciambelli P., Senatore A., Petrone V., 2013, New 'chimie douce' approach to the synthesis of hybrid nanosheets of MoS2 on CNT and their anti-friction and anti-wear properties, Nanotechnology 24, 125601 (11pp).

Alvarez L., Berhault G., Alonso-Nunez G., 2008, Unsupported NiMo Sulfide Catalysts Obtained from Nickel/Ammonium and Nickel/Tetraalkylammonium Thiomolybdates: Synthesis and Application in the Hydrodesulfurization of Dibenzothiophene, Catal. Lett. 45, 125-135

Casiraghi C., Ferrari A.C., Robertson J., 2005, Raman spectroscopy of hydrogenated amorphous carbons, Phys. Rev. B 72, 085401 (14pp).

Cervantes-Gaxiola M. E., Arroyo-Albiter M., Pérez-Larios A., Balbuena P. B., Espino-Valencia J., 2013, Experimental and theoretical study of NiMoW, NiMo, and NiW sulfide catalysts supported on an AlATiAMg mixed oxide during the hydrodesulfurization of dibenzothiophene, Fuel 113, 733–743.

Guillaume F., Huang S., Harris K. D.M., Couzi M., Talaga D., 2008, Optical phonons in millerite (NiS) from single-crystal polarized Raman spectroscopy, J. Raman Spectrosc. 39, 1419–1422.

Hernandez Y., Nicolosi V., Lotya M., Blighe F.M., Sun Z., De S., McGovern I.T., Holland B., Byrne M., Gun'ko Y.K., Boland J.J., Niraj P., Duesberg G., Krishnamurthy S., Goodhue R., Hutchison J., Scardaci V., Ferrari A.C., Coleman J.N., 2008, High-yield production of graphene by liquid-phase exfoliation of graphite, Nat. Nanotechnol. 3, 563-568.

Kou R., Shao Y., Mei D., Nie Z., Wang D., Wang C., Viswanathan V.V., Park S., Aksay I.A., Lin Y., Wang Y., Liu J., 2011, Stabilization of electrocatalytic metal nanoparticles at metal-metal oxide-graphene triple junction points. J. Am. Chem. Soc. 133, 2541–2547.

Li Y., Wang H., Xie L., Liang Y., Hong G., Dai H., 2011, MoS2 Nanoparticles Grown on Graphene: An Advanced Catalyst fort he Hydrogen Evolution Reaction, J. Am. Chem. Soc. 133, 7296-7299.

Pedraza F., Fuentes S., 2000, Ni–Mo and Ni–W sulfide catalysts prepared by decomposition of binary thiometallates Catal. Lett. 65, 107–113

Popczun E. J., McKone J.R.,. Read C.G., Biacchi A.J., Wiltrout A.M., Lewis N.S., Schaak R.E., 2013, Nanostructured nickel phosphide as an electrocatalyst for the hydrogen evolution reaction, J. Am. Chem. Soc. 135, 9267–9270.

Sarno M., Cirillo C., Piscitelli R., Ciambelli P., 2013, A study of the key parameters, including the crucial role of H2 for uniform graphene growth on Ni foil, J. Mol. Catal. A: Chem. 366, 303-314.

Sarno M., Garamella A., Cirillo C., Ciambelli P., 2014a, MoO2 synthesis for LIBs, Chem. Eng. Trans., submitted.

Sarno M., Garamella A., Cirillo C., Ciambelli P., 2014a, MoS2/MoO2/graphene electrocatalyst for HER, Chem. Eng. Trans., submitted.

Zhao Y., Zhang Y., Yang Z., Yan Y., Sun K., 2013, Synthesis of MoS2 and MoO2 for their applications in H2 generation and lithium ion batteries: a review, Sci. Technol. Adv. Mater. 14, 043501 (12pp).